

# Transcorrelated Theory with Pseudopotentials

Kristoffer Simula,<sup>\*,†</sup> Evelin Martine Corvid Christlmaier,<sup>†</sup> Maria-Andreea Filip,<sup>†</sup>

J. Philip Haupt,<sup>†</sup> Daniel Kats,<sup>†</sup> Pablo Lopez-Rios,<sup>†</sup> and Ali Alavi<sup>\*,†,‡</sup>

<sup>†</sup>*Max Planck Institute for Solid State Research, Heisenbergstr. 1, 70569 Stuttgart, Germany*

<sup>‡</sup>*Yusuf Hamied Department of Chemistry, University of Cambridge, Lensfield Road,  
Cambridge CB2 1EW, United Kingdom*

E-mail: k.simula@fkf.mpg.de; a.alavi@fkf.mpg.de

## Abstract

The transcorrelated (TC) method performs a similarity transformation on the electronic Schrödinger equation via Jastrow factorization of the wave function. This has demonstrated significant advancements in computational electronic structure theory by improving basis set convergence and compactifying the description of the wave function. In this work, we introduce a new approach that incorporates pseudopotentials (PPs) into the TC framework, significantly accelerating Jastrow factor optimization and reducing computational costs. Our results for ionization potentials, atomization energies, and dissociation curves of first-row atoms and molecules show that PPs provide chemically accurate descriptions across a range of systems and give guidelines for future theory and applications. The new pseudopotential-based TC method opens possibilities for applying TC to more complex and larger systems, such as transition metals and solid-state systems.

# Introduction

In methods based on electronic structure theory, solutions to the Schrödinger equation require simultaneous convergence with respect to basis sets and the treatment of electron correlation. Current *ab initio* methods that treat the electron correlation explicitly can achieve this accurately only for very small systems, due to the high polynomial or even exponential scaling of the computational cost with the number of electrons.

First quantized methods, such as Variational and Diffusion Monte Carlo (VMC and DMC), work in continuum space, circumventing the basis set issue. However, their accuracy is limited by the quality of the trial wave function. Systematic improvement of the wave function requires methods capable of treating electron correlation effectively.

Conversely, methods such as Coupled Cluster (CC) and configuration interaction (CI), formulated under the framework of second quantization, can often treat electron correlation accurately, but convergence to the basis set limit remains infeasible in many cases. Additionally, the divergent nature of the Coulomb interaction introduces sharp features, or cusps,<sup>1</sup> in the wave function, which are difficult to describe using determinants composed of smooth Gaussian-type orbitals, which are often used in second-quantized post-Hartree-Fock methods.

These issues of second quantization have been alleviated by explicitly correlated methods, which introduce interelectronic distance dependency in the system description. This is done to reduce basis set errors and account for the cusps, and to describe short-range electronic interactions without requiring a large number of determinants.

R12/F12 methods<sup>2,3</sup> have been widely applied in quantum chemistry to address these problems, and have been used in perturbation theory, coupled cluster, and configuration interaction calculations,<sup>4-6</sup> generally with good results.

The transcorrelated (TC) method is an explicitly correlated method that has seen rapid development in recent years.<sup>7-12</sup> TC takes a Jastrow factor, a function of interelectronic distances optimized in a first-quantized VMC calculation, and uses it to perform a similarity

transformation on the second-quantized Hamiltonian. This transformation preserves the Hamiltonian’s eigenvalues while addressing the cusps and significantly improving basis set convergence,<sup>13</sup> as well as compactifying the wave function.<sup>12,14</sup> Although the transformation introduces challenging three-body terms, a recent approximation, xTC,<sup>15</sup> removes the need to explicitly treat these terms, reducing the scaling in evaluation of the transcorrelated Hamiltonian by two orders of magnitude.

TC has shown very promising results in homogeneous electron gas (HEG) systems,<sup>16,17</sup> and the Hubbard model.<sup>14</sup> It has also been applied to atoms and molecules with high accuracy using FCIQMC and CC methods.<sup>7,18–20</sup> TC has also been used to produce accurate results in simulations with quantum hardware, where the TC Hamiltonian enables the use of shallower circuit depths.<sup>21</sup>

One of the bottlenecks of TC and xTC has been the optimization of the Jastrow factor, as the variance of the VMC wave function increases rapidly with system size, driving up computational costs for sufficient accuracy. To extend TC and xTC to larger systems or solids, further developments are needed to reduce the costs of Jastrow optimization and the following post-Hartree-Fock calculations. The pseudopotential (PP) approximation offers a promising solution, as it reduces the number of electrons, eliminates electron-nucleus cusps, and significantly lowers the VMC variance.

In this work, we investigate the use of PPs in xTC methods. Replacement of the nucleus and the surrounding core electrons with PPs introduces terms in the Hamiltonian that do not commute with the Jastrow factor, complicating the similarity transformation. In Section 2, we present the theory of transcorrelation with PPs. In Section 3, we discuss the computational details of our calculations. Section 4 presents results on ionization potentials for first-row elements (Be–F), atomization energies for molecules (CN, CO, CF, N<sub>2</sub>, O<sub>2</sub>, F<sub>2</sub>, H<sub>2</sub>O, CO<sub>2</sub>), and dissociation curves for N<sub>2</sub> and F<sub>2</sub>. We show that PPs accelerate the optimization of the Jastrow factor and provide chemically accurate descriptions across a variety of systems and chemical environments.

# Theory

## Pseudopotential approximation

Within the PP approximation the Coulombic interactions between the valence electrons and the atomic nuclei and core electrons are replaced with effective potentials. The PPs are constructed to reproduce the valence electron wave functions outside of a core region. This means that the electron-nucleus term of the Hamiltonian  $\hat{H}_{\text{en}}$  is replaced by a sum over effective potentials  $\hat{V}_{\text{eff}}$  for each atom:

$$\hat{H}_{\text{en}} = \sum_I^M \sum_{i=1}^N \frac{Z_I}{|\mathbf{r}_i - \mathbf{R}_I|} \rightarrow \hat{H}_{\text{en}}^{\text{PP}} = \sum_I^M \sum_{j=1}^{N_v} \hat{V}_{\text{eff}}^I(|\mathbf{r}_j - \mathbf{R}_I|). \quad (1)$$

Above,  $Z$  is the nuclear charge,  $N$  ( $M$ ) is the number of electrons (atoms), and  $\mathbf{r}_i$  ( $\mathbf{R}_I$ ) is the position of the  $i$ -th electron ( $I$ -th atom) with respect to the origin. With PPs, the summation runs over  $N_v$  valence electrons.

In the theory that follows, we focus on the effective potential of a single atom ( $M = 1$ ) for to simplify presentation, but the extension to multiatom systems is straightforward.

Outside of the core region  $V_{\text{eff}}^I$  should mimic the potential felt by the valence electrons due to the nucleus and the core electrons. It should also reproduce the exact electronic wave function outside of the core region specified by a cutoff radius  $r_c$ .  $V_{\text{eff}}$  consists of a number of angular momentum channels, one local without spherical projections and one or more nonlocal channels:

$$\hat{V}_{\text{eff}}(r) = V_{l_{\text{max}}}(r) + \sum_{l=0}^{l_{\text{max}}-1} V_l(r) \sum_{m=-l}^l |Y_{lm}\rangle \langle Y_{lm}|. \quad (2)$$

Above,  $Y_{lm}$  are the spherical harmonics, and  $V_l(r)$  are the pseudopotential radial functions.  $l_{\text{max}}$  is the maximum angular momentum quantum number included in the PP, which is also

chosen as the local channel.  $V_l$  are expressed as:

$$V_l(r) = \begin{cases} -\frac{Z_{\text{eff}}}{r} \left(1 - e^{-\alpha r^2}\right) + \alpha Z_{\text{eff}} r e^{-\beta r^2} + \sum_{q=1}^n \gamma_{ql} e^{-\delta_{ql} r^2} & l = l_{\text{max}} \\ \sum_{q=1}^m \gamma_{ql} e^{-\delta_{ql} r^2} & l < l_{\text{max}} \end{cases} \quad (3)$$

We use two sets of PPs in this work: energy-consistent correlated electron PPs (eCEPPs) by Trail & Needs,<sup>22</sup> and correlation-consistent effective core potentials (ccECPs) by Lubos-Mitas<sup>23</sup> *et al.* The eCEPPs have  $l_{\text{max}} = 2$  for the first-row atoms, with  $n = 4$  and  $m = 6$ , while the ccECPs have  $l_{\text{max}} = 1$  and  $n = m = 1$ , leaving only one gaussian term for the non-local channels. The different components of ccECPs and eCEPPs for C, N, O, and F are shown in Fig. 1. In the figure, it can be seen that the eCEPPs have much smaller potential absolute values than the ccECPs.

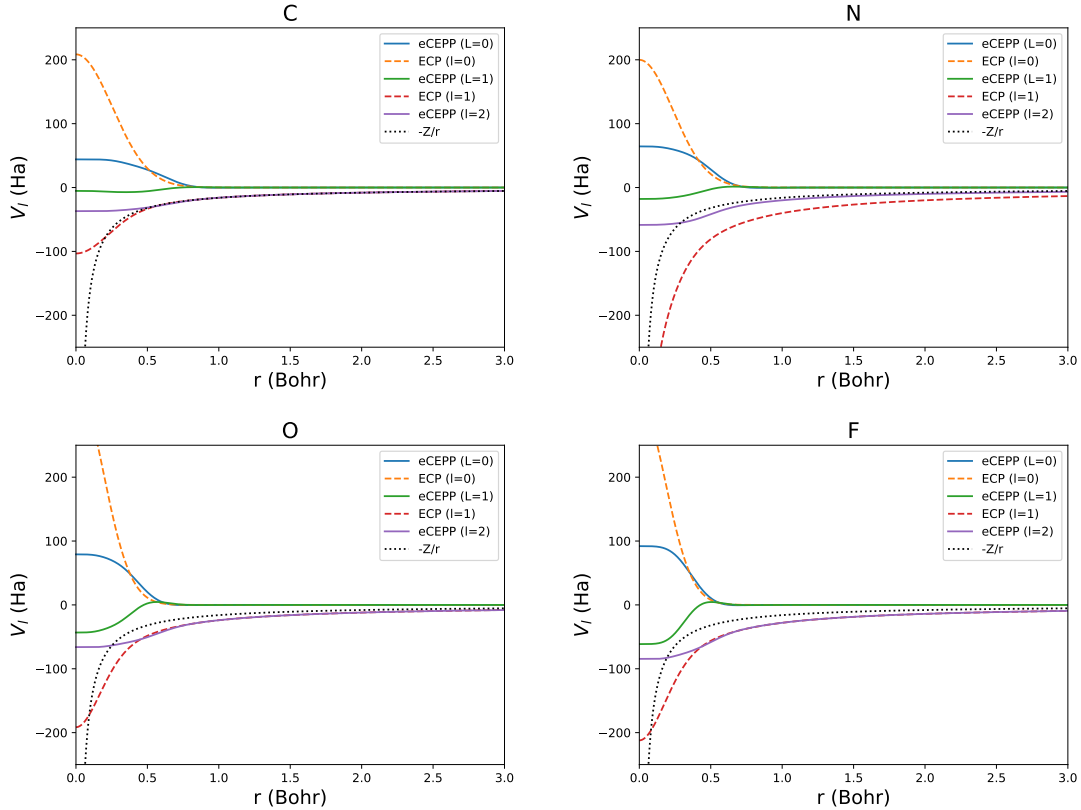


Figure 1:  $V_l(r)$  of eCEPPs (solid lines) and ccECPs (dashed lines) of C, N, O, and F. Black dashed lines show the Coulombic potential of the nucleus.

The action of  $\hat{V}_{\text{eff}}$  on a function  $f(\mathbf{r})$  (with or without a Jastrow factor) of the position of electron  $i$  is:

$$\hat{V}_{\text{eff}}(r_i)f(\mathbf{r}_i) = \sum_{l=0}^{l_{\text{max}}} V_l(r_i) \sum_{m=-l}^l Y_{lm}(\Omega_{\mathbf{r}_i}) \int_{|\mathbf{r}'|=r_i} d\Omega_{\mathbf{r}'} f(\mathbf{r}') Y_{lm}(\Omega_{\mathbf{r}'}). \quad (4)$$

Because  $Y_{lm}(f=0, \theta=0) = 0$  for  $m \neq 0$ , we can simplify this expression – by choosing the  $z$ -axis to be along  $\mathbf{r}_i$  – to:<sup>24</sup>

$$\hat{V}_{eff}(r_i)f(\mathbf{r}_i) = \sum_{l=0}^{l_{\text{max}}} V_l(r_i) Y_{l0}(\Omega_{\mathbf{r}_i}) \int_{|\mathbf{r}'|=r_i} d\Omega_{\mathbf{r}'} f(\mathbf{r}') Y_{l0}(\Omega_{\mathbf{r}'}), \quad (5)$$

which is the expression we use to estimate the action of the PP on the electronic orbitals and the Jastrow factor.

## Pseudopotentials in the Transcorrelated Hamiltonian

In transcorrelation theory, the Hamiltonian is supplemented with a Jastrow factor  $J$ , which is a function to describe interparticle correlations. With  $N$  electrons and  $M$  nuclei in a system, the Jastrow factor in this work is of Drummond-Towler-Needs (DNT) type:<sup>25</sup>

$$\begin{aligned} J(\{\mathbf{r}_i\}, \{\mathbf{R}_I\}) &= \sum_{I=1}^M \sum_{i=1}^N \chi(\mathbf{r}_{iI}) + \sum_{i<j} u(|\mathbf{r}_i - \mathbf{r}_j|) + \sum_{I=1}^M \sum_{i<j} f(\mathbf{r}_{iI}, \mathbf{r}_{jI}, |\mathbf{r}_i - \mathbf{r}_j|) \\ &= \sum_{I=1}^M \sum_{i>j} J_2(\mathbf{r}_i, \mathbf{r}_j; \mathbf{R}_I), \end{aligned} \quad (6)$$

including 1-body ( $\chi$ , electron-nucleus), 2-body ( $u$ , electron-electron), and 3-body ( $f$ , electron-electron-nucleus) terms. Each of the terms is optimized for interparticle distances under a chosen cutoff value, characteristic of the DNT Jastrow form. Above,  $\mathbf{r}_{iI} = \mathbf{r}_i - \mathbf{R}_I$ . In the above, in order to simplify the derivation of the pseudopotential commutator equations,<sup>15</sup> we have included all of the terms involving  $\chi$ ,  $u$  and  $f$  into the term  $J_2(\mathbf{r}_i, \mathbf{r}_j, \mathbf{R}_I)$ . This approach gives TC contributions to the 2- and 3-body terms  $\langle pr|qs \rangle$  and  $\langle pqr|stu \rangle$  of the

Hamiltonian, including also the  $\chi$ -term contribution to these terms. We call this approach the "combined" Jastrow treatment. Alternatively, one could treat the 1- and 2-body terms in the Jastrow factor separately (which we call the "separate" Jastrow treatment) and include the contribution of  $\chi$  into the 1-body terms  $\langle p|q \rangle$ . The separate Jastrow treatment does not remove the contribution of the  $\chi$ -term from the 2-body integrals, however, because of the presence of a cross-term (see Supplementary Material). With small  $\chi$  cutoff values the combined and separated treatments yield almost exactly the same coupled cluster total energies for atoms and molecules at equilibrium geometries, with discrepancy of  $< .1\text{mHa}$ . However, we found difficulties with the separated Jastrow treatment with PPs whenever the Jastrow cutoff values for the  $\chi$  functions exceeded the inter-nuclear bond lengths, and for this reason we chose the combined approach in this study. We present the equations for the separated treatment of the 1- and 2-body terms in the Jastrow factor in the Supplementary Material.

The transcorrelated Hamiltonian is obtained from a similarity transformation of the original Hamiltonian:

$$\hat{H}_{TC} = \exp(-J)\hat{H}\exp(J) = \hat{H} + [\hat{H}, J] + \frac{1}{2!}[[\hat{H}, J], J] + \dots \quad (7)$$

Any operator component of the Hamiltonian  $\hat{O}$  that does not commute with the Jastrow factor  $J$  will extend the transcorrelated Hamiltonian. For single-particle operators, the first two commutators can be expressed as:

$$\begin{aligned} [\hat{O}, J] &= \sum_{k=1}^N \sum_{i < j} \left[ \hat{O}(\mathbf{r}_k), \sum_I^M J_2(\mathbf{r}_i, \mathbf{r}_j; \mathbf{R}_I) \right] = \sum_{k=1}^N \sum_{i < j} \Pi_{ij}^k(\hat{O}), \\ [[\hat{O}, J], J] &= \sum_{k=1}^N \sum_{i < j} \sum_{l < m} \left[ \left[ \hat{O}(\mathbf{r}_k), \sum_I^M J_2(\mathbf{r}_i, \mathbf{r}_j; \mathbf{R}_I) \right], \sum_J^M J_2(\mathbf{r}_l, \mathbf{r}_m; \mathbf{R}_J) \right] = \sum_{k=1}^N \sum_{i < j} \sum_{l < m} \Gamma_{ijlm}^k(\hat{O}). \end{aligned} \quad (8)$$

It should be noted that the similarity transformation breaks the variational principle, al-

though it does not affect the eigenvalues of the Hamiltonian.

There are restrictions to the indexing of  $\Pi$  and  $\Gamma$  terms. First,  $\Pi_{ij}^k$  is non-zero only when  $k = i$  or  $k = j$ . Second,  $\Gamma_{ijlm}^k$  is non-zero only when  $k = i$  and  $i \in (l, m)$  or  $k = j$  and  $j \in (l, m)$ . Hence the commutators can be expressed as:

$$\begin{aligned} [\hat{O}, J] &= \sum_{i < j} \Pi_{ij}^i(\hat{O}) + \Pi_{ij}^j(\hat{O}), \\ [[\hat{O}, J], J] &= \sum_{i > j} \left[ \Gamma_{ijij}^i(\hat{O}) + \Gamma_{ijij}^j(\hat{O}) \right] \\ &\quad + \sum_{i > j > m} \left[ \Gamma_{ijim}^i(\hat{O}) + \Gamma_{ijim}^j(\hat{O}) + \Gamma_{mimj}^m(\hat{O}) \right]. \end{aligned} \quad (9)$$

In all-electron transcorrelation theory, the only component of the Hamiltonian that does not commute with the Jastrow factor is the kinetic energy operator.<sup>7</sup> In this case the similarity transformation of Eq. (7) terminates exactly at the second commutator, and the transcorrelated Hamiltonian is computed with the commutators in Eq. (9), introducing 2- and 3-body terms in the Hamiltonian.

With PPs, the  $V_{\text{eff}}$  terms do not commute with the Jastrow factor. In addition, commutator summation in the similarity transformation is not guaranteed to terminate at the second commutator. To estimate the effect of the PP on the transcorrelated Hamiltonian, we make an approximation of only considering the 2-body terms of the PP commutators, ignoring the sum over  $i > j > m$  in Eq. (9). This approximation is made under the assumption that the 3-body interactions of the valence electrons close to the core are negligible. Explicit treatment of the 3-body terms, possibly under the xTC approximation, is left for future work in case it is needed. Within this approximation, the transcorrelated second-quantized Hamiltonian becomes

$$\begin{aligned} \hat{H} &= \sum_{pq\sigma} h_q^p a_{p\sigma}^\dagger a_{q\sigma} + \frac{1}{2} \sum_{pqrs} (V_{rs}^{pq} - K_{rs}^{pq} + P_{rs}^{pq}) \sum_{\sigma\tau} a_{p\sigma}^\dagger a_{q\tau}^\dagger a_{r\tau} a_{s\sigma} \\ &\quad - \frac{1}{6} \sum_{pqrstu} L_{stu}^{pqr} \sum_{\sigma\tau\lambda} a_{p\sigma}^\dagger a_{q\sigma'}^\dagger a_{r\lambda}^\dagger a_{s\lambda} a_{t\tau} a_{u\sigma}. \end{aligned} \quad (10)$$



The terms  $h$  and  $V$  are traditional one- and two-body terms of the second-quantized Hamiltonian, while the calculation of the transcorrelated components  $K$  and  $L$  arising from the kinetic energy operator has been described elsewhere.<sup>7,15</sup> The pseudopotential terms  $P$  are computed as:

$$P_{rs}^{pq} = \left\langle \phi_p \phi_q \left| \Pi_{12}^1(\hat{H}_{\text{en}}^{\text{PP}}) + \Pi_{12}^2(\hat{H}_{\text{en}}^{\text{PP}}) + \frac{1}{2}\Gamma_{1212}^1(\hat{H}_{\text{en}}^{\text{PP}}) + \frac{1}{2}\Gamma_{1212}^2(\hat{H}_{\text{en}}^{\text{PP}}) \right| \phi_r \phi_s \right\rangle \quad (11)$$

with

$$\begin{aligned} \Pi_{ij}^i(\hat{H}_{\text{en}}^{\text{PP}}) &= \sum_I^M \left[ \hat{H}_{\text{en}}^{\text{PP}}(\mathbf{r}_i) J_2(\mathbf{r}_i, \mathbf{r}_j; \mathbf{R}_I) - J_2(\mathbf{r}_i, \mathbf{r}_j; \mathbf{R}_I) \hat{H}_{\text{en}}^{\text{PP}}(\mathbf{r}_i) \right], \\ \Gamma_{ijij}^i(\hat{H}_{\text{en}}^{\text{PP}}) &= \hat{H}_{\text{en}}^{\text{PP}}(\mathbf{r}_i) \left[ \sum_I^M J_2(\mathbf{r}_i, \mathbf{r}_j; \mathbf{R}_I) \right]^2 - 2 \sum_I^M J_2(\mathbf{r}_i, \mathbf{r}_j; \mathbf{R}_I) \hat{H}_{\text{en}}^{\text{PP}}(\mathbf{r}_i) \sum_J^M J_2(\mathbf{r}_i, \mathbf{r}_j; \mathbf{R}_J) \\ &\quad + \left[ \sum_I^M J_2(\mathbf{r}_i, \mathbf{r}_j; \mathbf{R}_I) \right]^2 \hat{H}_{\text{en}}^{\text{PP}}(\mathbf{r}_i). \end{aligned} \quad (12)$$

Therefore, in order to evaluate the PP commutators (under the present approximation of restricting ccECP corrections to two-body terms) in Eq. (11), we need to apply Eq. (5) to calculate terms of the type  $\hat{H}_{\text{en}}^{\text{PP}}\phi$ ,  $\hat{H}_{\text{en}}^{\text{PP}}J_2\phi$ , and  $\hat{H}_{\text{en}}^{\text{PP}}J_2^2\phi$ . This allows us to construct the transcorrelated Hamiltonian in Eq. (10). We have included also higher-order terms in the PP commutators in Eq. (12) in our calculations, under the assumption that the 3-body terms are negligible.

## Calculations

### Evaluation of transcorrelated Hamiltonian with pseudopotentials

The transcorrelated second-quantized Hamiltonians are calculated with an in-house code TCHINT,<sup>26</sup> that is based on the version used in.<sup>7</sup> TCHINT calculates transcorrelated second-

quantized Hamiltonians with a Jastrow factor and the molecular orbitals as inputs. It is parallelized with MPI, uses the BLAS and LAPACK libraries for matrix operations, and is written in Fortran. The inclusion of the features necessary for the PP commutator evaluation within TCHINT has been an important part of this work.

The elements  $P_{rs}^{pq}$  in Eq. (11) are obtained with numerical integration over real-space grid points. The operation of  $\hat{H}_{\text{en}}^{\text{PP}}$  in terms  $\Pi$  and  $\Gamma$  is evaluated according to Eq. (5), by discretizing the spherical integration, so that

$$\hat{V}_{\text{eff}}(r_i)f(\mathbf{r}_i) = \sum_{l=0}^{l_{\text{max}}} V_l(r_i)Y_{l0}(\Omega_{\mathbf{r}_i}) \sum_{i=1}^{N_s} f(\mathbf{r}_i')Y_{l0}(\Omega_{\mathbf{r}_i'}), \quad (13)$$

where  $|\mathbf{r}_i'| = |\mathbf{r}_i| = r_i$  and  $f$  is either  $\phi_r(\mathbf{r}_1)$ ,  $J_2(\mathbf{r}_1, \mathbf{r}_2)\phi_r(\mathbf{r}_1)$ , or  $J_2(\mathbf{r}_1, \mathbf{r}_2)^2\phi_r(\mathbf{r}_1)$ . The spherical grid points are chosen as the vertices of an icosahedron. The points are obtained by setting them on unit sphere scaled with  $r_i$ , so that  $[\pm a, \pm b, 0]$ ,  $[\pm b, \pm a, 0]$ , and  $[0, \pm a, \pm b]$  are the grid points  $\mathbf{r}_i'$  on the unit sphere, with  $a = r_i/\sqrt{1+\phi^2}$  and  $b = \phi r_i/\sqrt{1+\phi^2}$ , where  $\phi = (1 + \sqrt{5})/2$  is the golden ratio. Hence  $N_s = 12$ . This is a Lebedev grid capable of exact spherical integration of functions that have up to  $l = 5$  components. Tests on denser spherical grids did not change the results significantly. To mitigate the bias by the orientation of the spherical grid we applied random rotations to the spherical grid points in each spherical projection.

For a number of grid points  $N_{\text{ECP}}$  under pseudopotential influence, the numbers of additional Jastrow factor and orbital evaluations due to presence of pseudopotentials are  $N_g N_{\text{ECP}} N_s$  and  $N_{\text{ECP}} N_{\text{orb}} N_s$ , respectively, where  $N_g$  is the total number of grid points and  $N_{\text{orb}}$  is the number of orbitals. The additional jastrow evaluations thus add a  $N_{\text{ECP}} N_s / N_g$  prefactor to the computational scaling of the Jastrow evaluations,<sup>7</sup> which is computationally most expensive part of the calculation. To mitigate the additional computational cost and load imbalance, we use vectorized Jastrow evaluations and a load balancing scheme that distributes the grid points evenly among the MPI processes. Orbitals at the spherical

grid points are evaluated at the beginning of the calculation, and the memory requirements are increased because of ECPs by additional  $N_{\text{ECP}}N_{\text{orb}}N_{\text{s}}$  orbital floating point numbers as opposed to the  $N_{\text{g}}N_{\text{orb}}$  floating point numbers required for all-electron calculations.

Table 1 shows a list of the number of grid points under pseudopotential influence for a number of systems studied in this work. For each system, the number of grid points is roughly 55% of the total number of grid points.

Table 1: Total and ECP-influenced grid points for each system and pseudopotential.

System	Total	eCEPP	ccECP
C	18120	10570	10268
N	18120	10570	9966
O	18120	10268	9362
F	18120	9966	9060
N <sub>2</sub>	36196	22792	20810
O <sub>2</sub>	36198	21380	19058
F <sub>2</sub>	36202	20316	18324
CN	36196	22445	21045
CO	36196	22022	20313
CF	36198	21299	19767
H <sub>2</sub> O	33484	20066	9612
CO <sub>2</sub>	54056	33384	30250

The treatment of the 3-body terms when constructing the transcorrelated Hamiltonian is done under the xTC approximation.<sup>15</sup> In this approximation, the last term of Eq. 10 containing  $L$  is reorganized within the generalized normal ordering scheme. This leads to modifications in the 1-,2-, and 3-body terms of the transcorrelated Hamiltonian. The contributions of the 3-body terms under the generalized normal ordering to the 1- and 2-body terms are evaluated by contracting the 3-body terms with the reduced 1-body density matrix of the Hartree-Fock wave function (with the exception of using FCI density matrix in the N<sub>2</sub> dissociation curve calculations. The remaining 3-body terms are neglected in xTC.

## General computational details

In this work we study the use of pseudopotentials with the transcorrelated Hamiltonian in atoms Be, B, C, N, O, and F, as well as their +1 ions. We also study the total and atomization energies of molecules CN, CO, CF, N<sub>2</sub>, O<sub>2</sub>, F<sub>2</sub>, H<sub>2</sub>O and CO<sub>2</sub>. We use the aug-cc-pVD/T/QZ

basis sets (AVXZ, with X=D,T,Q), optimized individually for each pseudopotential.<sup>22,23</sup> Ionization energies with ccECPs are evaluated with non-augmented cc-pVD/T/QZ basis sets (PVXZ, with X=D,T,Q). .

The geometries of the molecules are taken from those in the HEAT database.<sup>27</sup> The Hartree-Fock (HF) calculations are done with the PYSCF code.<sup>28</sup> The Jastrow factors used are of Drummond-Towler-Needs type<sup>25</sup> and are optimised with respect to the variance of the Hartree-Fock wave function using the VMC method of the CASINO package.<sup>29</sup> The Jastrow factors are optimized separately for each system, basis set, and pseudopotential combination. The cutoffs used for the  $u$ ,  $\chi$ , and  $f$  terms were 4.5, 4, and 4, respectively. We provide the optimized Jastrow factors in the Supplementary Material.

The atomization energies are calculated both with and without transcorrelation with the coupled cluster using singles, doubles and perturbative and full triples (CCSD(T) and CCSDT) using the ElemCo.jl package.<sup>30</sup> If transcorrelation is used, we add a prefix xTC- to the method name. The similarity transformation of the Hamiltonian using the Jastrow factor leads to a non-Hermitian Hamiltonian with a non-diagonal Fock matrix. Consequently, standard non-iterative perturbative methods for CCSD(T) are not directly applicable to the transcorrelated Hamiltonian. Thus for transcorrelated CCSD(T) we do the calculations with a pseudocanonical ACCSD(T) approach using bi-orthogonal orbitals.<sup>31</sup> To simplify notation we will call it xTC-CCSD(T).

The atomization energies are also calculated with CCSD(T)-F12 using the Molpro package<sup>32-34</sup> for comparison. Both all-electron and PP F12 results are calculated to assess the effect of the PPs on the results. In all-electron calculations we use the standard AVXZ family of basis sets with AVXZ-MP2Fit and VXZ-JKFit auxiliary basis sets.<sup>35</sup> In PP calculations we use the augmented basis sets fitted for PPs.<sup>22,23</sup> As the auxiliary basis sets with PPs we use mp2-fitted QZVPP/MP2Fit and TZVPP/MP2Fit basis sets.

For the dissociation curves, we use the full configuration interaction quantum Monte Carlo method (FCIQMC)<sup>36</sup> with the NECI package<sup>37</sup> both with and without transcorrelated

Hamiltonians. The initiator approximation<sup>36</sup> with an initiator threshold of 3 is used in the FCIQMC calculations. The walker number for each calculation was increased by a factor of 5 until the energy was converged to within 1 mHa. We compare the results with MRCI-F12 calculations, done with the Molpro package.<sup>32–34</sup> The Davidson correction<sup>38</sup> is used in the MRCI-F12 calculations.

## Notation

All of the calculations presented in the following sections – with the exception of some of the F12-calculations – are done with PPs. To estimate the effect of evaluating the PP commutators we do the transcorrelated calculations without the PP commutators, and with varying level of commutator evaluations. We refer to these calculations as xTC-{method}(PP-n), with n indicating the level of commutator evaluation (0 – 4 commutator evaluations in this work) and method indicating the method used (CCSD(T), CCSDT, FCIQMC).

When presenting the total energies of atoms, ions, and molecules with PPs, we show the results relative to an energy  $E_{\text{CBS}}^{\text{TZ-QZ}}$ , evaluated as the sum of Hartree-Fock energy in the PVQZ (ccECPs) or AVQZ (eCEPPs) basis set,  $E_{\text{HF}}^{\text{QZ}}$ , and the estimate of the complete basis set limit (CBS) of CCSD(T) correlation energy. This estimate is obtained from the PVTZ and PVQZ (ECP) or AVTZ and AVQZ (eCEPP) correlation energies  $E_{\text{TZ}}^{\text{Corr}}(\text{CCSD(T)})$  and  $E_{\text{QZ}}^{\text{Corr}}(\text{CCSD(T)})$  with a linear extrapolation, so that

$$E_{\text{CBS}}^{\text{TZ-QZ}}(\text{CCSD(T)}) = E_{\text{HF}}^{\text{QZ}} + \frac{3^3 E_{\text{TZ}}^{\text{Corr}}(\text{CCSD(T)}) - 4^3 E_{\text{QZ}}^{\text{Corr}}(\text{CCSD(T)})}{3^3 - 4^3}. \quad (14)$$

This estimation of the complete basis set limit energy with respect to the triple- and quadruple-zeta basis sets is not meant to serve as a benchmark, but rather as a reference point for the PP energies for easier comparison.

# Results

## Variances in VMC optimization

Table 2 shows the variance of the reference energy in Hartrees for the first row elements Be-F, and for a set of first row molecules, obtained from eCEPP, ccECP, and all-electron (AE) calculations. For the results, we sampled the reference Hartree-Fock wave function with the Metropolis algorithm and evaluated an estimate of the variance of the obtained configurations together with the optimized Jastrow factor. The percentages after the PP variances show the ratio of PP values against the all-electron variances. The variance is significantly reduced when using PPs as compared to AE calculations. The variance reduction is greater for the heavier atoms. For the atoms, the variance reduction seems to obey roughly  $1/N_v$  dependence, where  $N_v$  is the number of valence electrons.

The non-local PP cutoff is generally lower for ccECPs than for eCEPPs (see Table 3). With the ccECPs and eCEPPs we got almost identical variances, which hints that the variance is stable against the cutoff radius.

Table 2: Variance data for atoms and molecules using AE, eCEPP, and ccECP methods. Units are in Hartrees. The percentages after the PP variances show the ratio of PP values against the all-electron variances.

Atom/Molecule	AE	eCEPP	ccECP
<b>Be</b>	0.0586	0.0146 (25%)	0.0180 (31%)
<b>B</b>	0.224	0.045 (20%)	0.049 (22%)
<b>C</b>	0.510	0.085 (17%)	0.082 (16%)
<b>N</b>	1.110	0.144 (13%)	0.135 (12%)
<b>O</b>	2.290	0.254 (11%)	0.243 (11%)
<b>F</b>	4.300	0.400 (9%)	0.364 (8%)
<b>N<sub>2</sub></b>	2.067	0.4441 (21%)	0.4313 (21%)
<b>O<sub>2</sub></b>	3.734	0.7133 (19%)	0.6741 (18%)
<b>F<sub>2</sub></b>	6.428	0.9423 (15%)	0.8828 (14%)
<b>CN</b>	1.482	0.3353 (23%)	0.3188 (22%)
<b>CF</b>	3.753	0.5674 (15%)	0.5336 (14%)
<b>CO</b>	2.483	0.4602 (19%)	0.4321 (17%)
<b>H<sub>2</sub>O</b>	1.763	0.3100 (18%)	0.2917 (17%)
<b>CO<sub>2</sub></b>	4.236	0.7683 (18%)	0.7212 (17%)

Table 3: Non-local cutoff radius values (Bohr) for various atoms, in atomic units, for eCEPPs and ccECPs. The cutoff is defined as the radius above which the PP radial functions are less than  $10^{-6}$  Ha.

Atom	Be	B	C	N	O	F
<b>eCEPP</b>	2.735610	2.066929	1.603693	1.608516	1.427703	1.324644
<b>ccECP</b>	2.405539	1.897133	1.430486	1.341815	1.088303	1.039012

Because the variance of the VMC energy is smaller with PPs, one can optimize the Jastrow factor with fewer Monte Carlo samples and hence less computational cost.

## Analysis of the transcorrelated integrals

For the systems studied in this work, we have investigated statistical parameters of the off-diagonal values of  $V$ ,  $K$ , and  $P$  tensors, as well as the full TC Hamiltonian. The minima, maximas, mean values, and Frobenius norms of the tensors are shown in Fig. 2 for both ccECPs and eCEPPs. The values are shown in Hartrees. Frobenius norm is defined as  $F = \sqrt{\sum_{ij} A_{ij}^2}$  for a matrix  $A$ .

The data shows that the largest values and overall weight of the off-diagonals are in the  $V$  tensor, i.e., the non-transcorrelated Hamiltonian, with the full TC Hamiltonian having slightly smaller values and overall weight (the Frobenius norm) than  $V$ . The  $K$  tensor of the kinetic energy operator commutators has much smaller weight compared to the full Hamiltonian, and the statistical parameters of the  $P$  tensor show that the pseudopotential commutators introduce only a slight correction to the TC Hamiltonian.

This data shows that pseudopotential commutators introduce generally small but non-negligible contributions.

## TC Hamiltonian Statistics

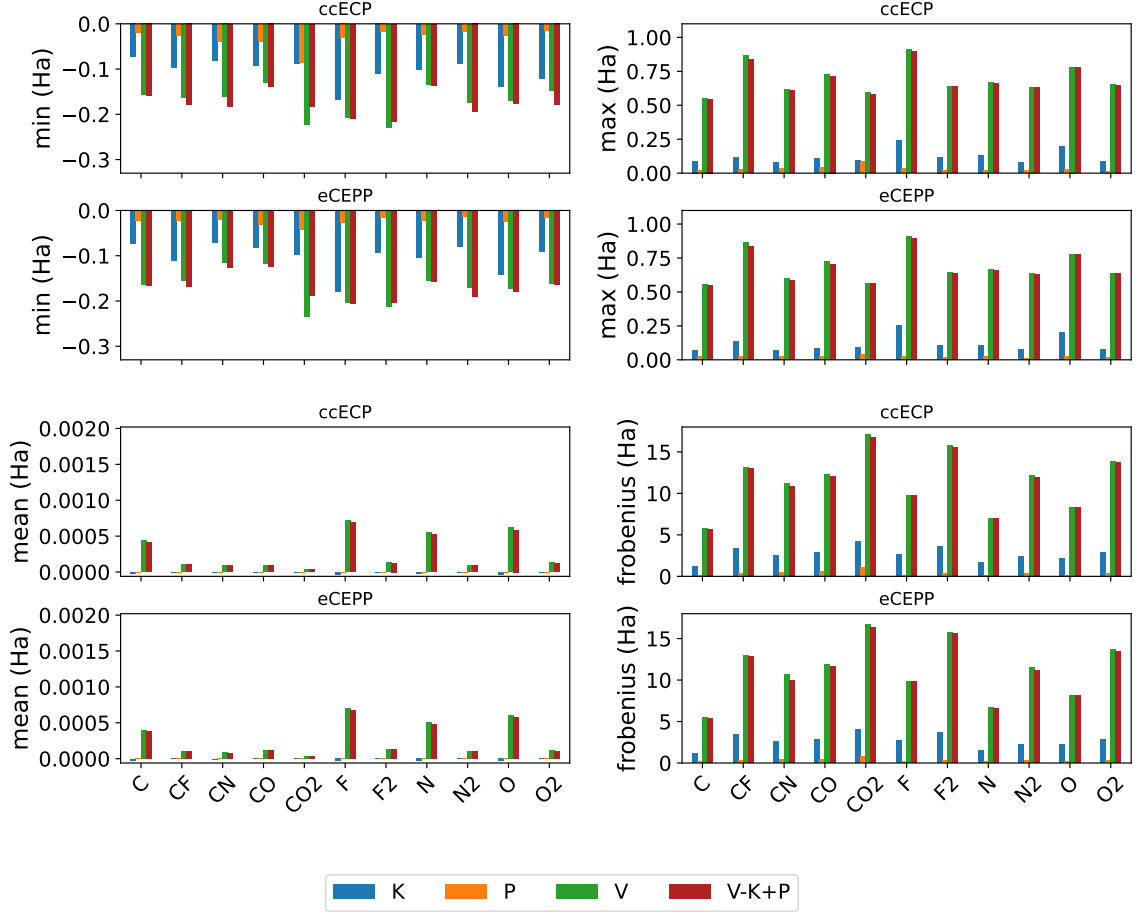


Figure 2: Parameters of the off-diagonal values of  $V$  (green),  $K$  (blue),  $P$  (orange), and  $V - K + P$  (red) tensors of Eq. 10 for different systems. The minima (upper left), maximas (upper right), mean values (lower left), and Frobenius norms (lower right) of the tensors are shown in Hartrees. For each stochastic parameter, we show values for each system for both ccECPs and eCEPPs.



# Atoms Be-F

## Analysis of the degree of PP commutators

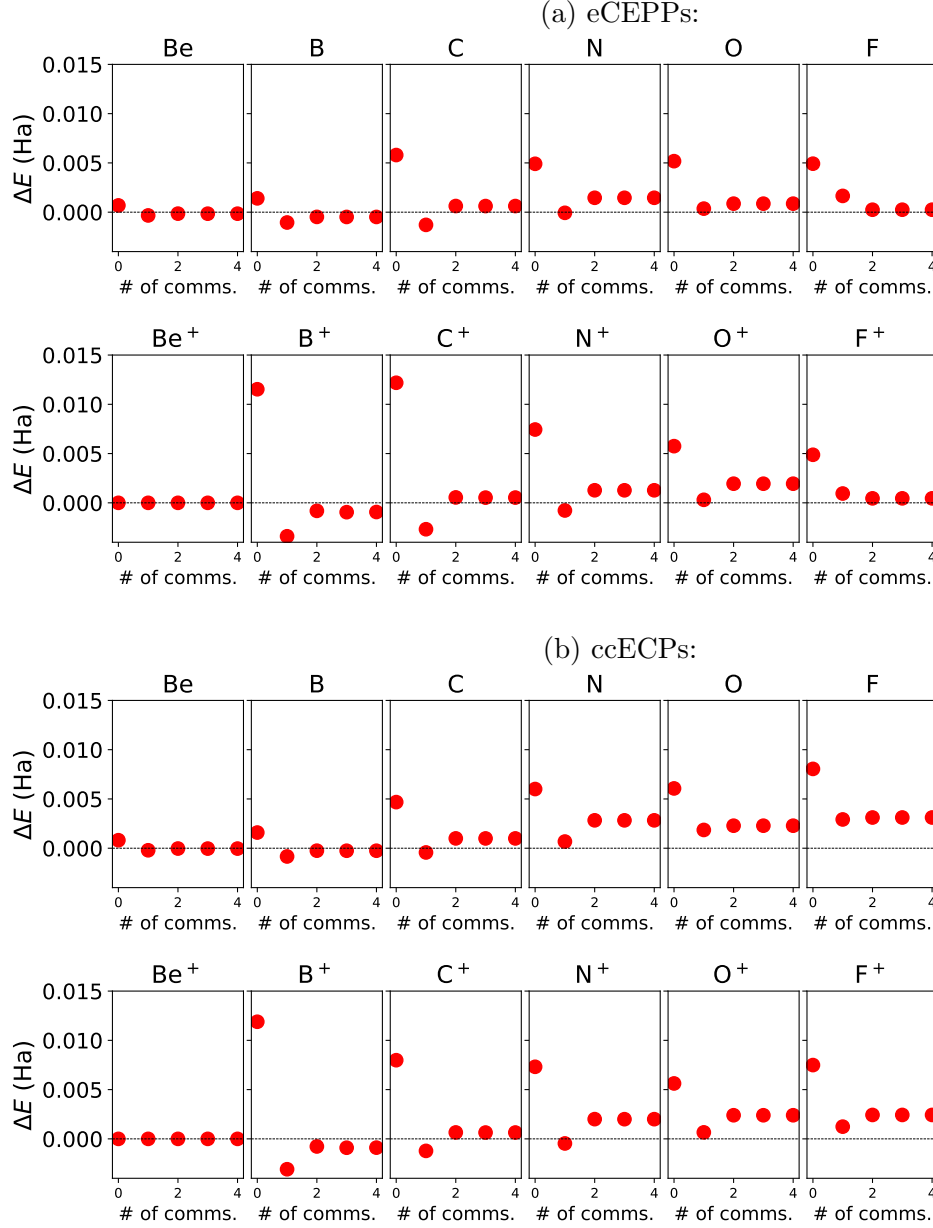


Figure 3: xTC-CCSD(T)(PP- $n$ ) energies with eCEPPs (figure (a), AVQZ basis) and ccECPs (figure (b), PVQZ basis) for the neutral and ionised states of the first row elements considered, shown as a function of the degree of PP commutators  $n$ . Results with  $n = 0, 1, 2, 3, 4$  are shown. Results are presented relative to CBS estimate as  $\Delta E = E(\text{xTC-CCSD(T)(PP-}n)) - E_{\text{CBS}}^{\text{TZ-QZ}}(\text{CCSD(T)})$ , see Eq. (14)

In Fig. 3 we show the xTC-CCSD(T)(PP- $n$ ) total energies of the first row elements Be-F, along with their ionised states, as a function of  $n$ , the degree of PP commutators evaluated. Results with both eCEPPs (a) and ccECPs (b) are shown. The results are calculated with the quadruple-zeta basis set. The zero in the y-axis refers to  $E_{\text{CBS}}^{\text{TZ-QZ}}(\text{CCSD(T)})$  (see Eq. (14)).

The Be cation with PPs has only one electron, and hence there is no correlation energy. With other atoms and ions, the general trend is that the xTC-CCSD(T)(PP-1) are smaller than the xTC-CCSD(T)(PP-0) energies, and the xTC-CCSD(T)(PP-2) energies increase slightly from the xTC-CCSD(T)(PP-1) energies. The energy converges with the 2nd order commutator evaluation for all of the systems, except for the B ion, where the 3rd order commutator evaluation still decreases the energy, although the difference is small.

Figure 4 shows the ionisation energies of the first row elements Be-F, obtained with CCSD(T), xTC-CCSD(T)(PP-0), xTC-CCSD(T)(PP-1), and xTC-CCSD(T)(PP-2) using both eCEPPs (a) and ccECPs (b). The results are shown as a function of the basis set. The ionisation energies are shown against experimental values.<sup>39</sup>

CCSD(T) ionisation energies reach chemical accuracy (1.6mHa, 0.04eV) for Be, C, and N with ccECPs and PVQZ basis set. With eCEPPs and AVQZ basis only Be ionisation energy with CCSD(T) is chemically accurate, but B, C, and N are close to chemical accuracy.

With xTC-CCSD(T)(PP-2) we reach chemical accuracy already with the AVTZ basis set for all of the atoms, with both PPs. The evaluation of the PP commutators is seen to be important, as with PP commutator degrees  $n < 2$  the xTC-CCSD(T)(PP- $n$ ) ionisation energies are generally worse.

Table 4 shows the mean absolute and root mean square errors (MAE and RMS) of the ionisation energies, evaluated against experimental values, of the first row elements Be-F, obtained with CCSD(T) and xTC-CCSD(T)(PP- $n$ ) methods and  $n = 0 - 4$ . The errors are averaged over the 1st-row atoms studied, and are shown separately for each basis set. Results are shown for both eCEPPs and ccECPs.

Table 4 shows that CCSD(T), xTC-CCSD(T)(PP-0), and xTC-CCSD(T)(PP-1) methods do not reach chemical accuracy with respect to MAE and RMS for the ionisation energies of the first row elements with any of the basis sets. xTC-CCSD(T)(PP-0) is even worse in accuracy than CCSD(T) in quadruple-zeta basis sets. However, xTC-CCSD(T)(PP-2) reaches chemical accuracy for both the MAE and MSE with both of the PPs at triple and quadruple-zeta basis sets.

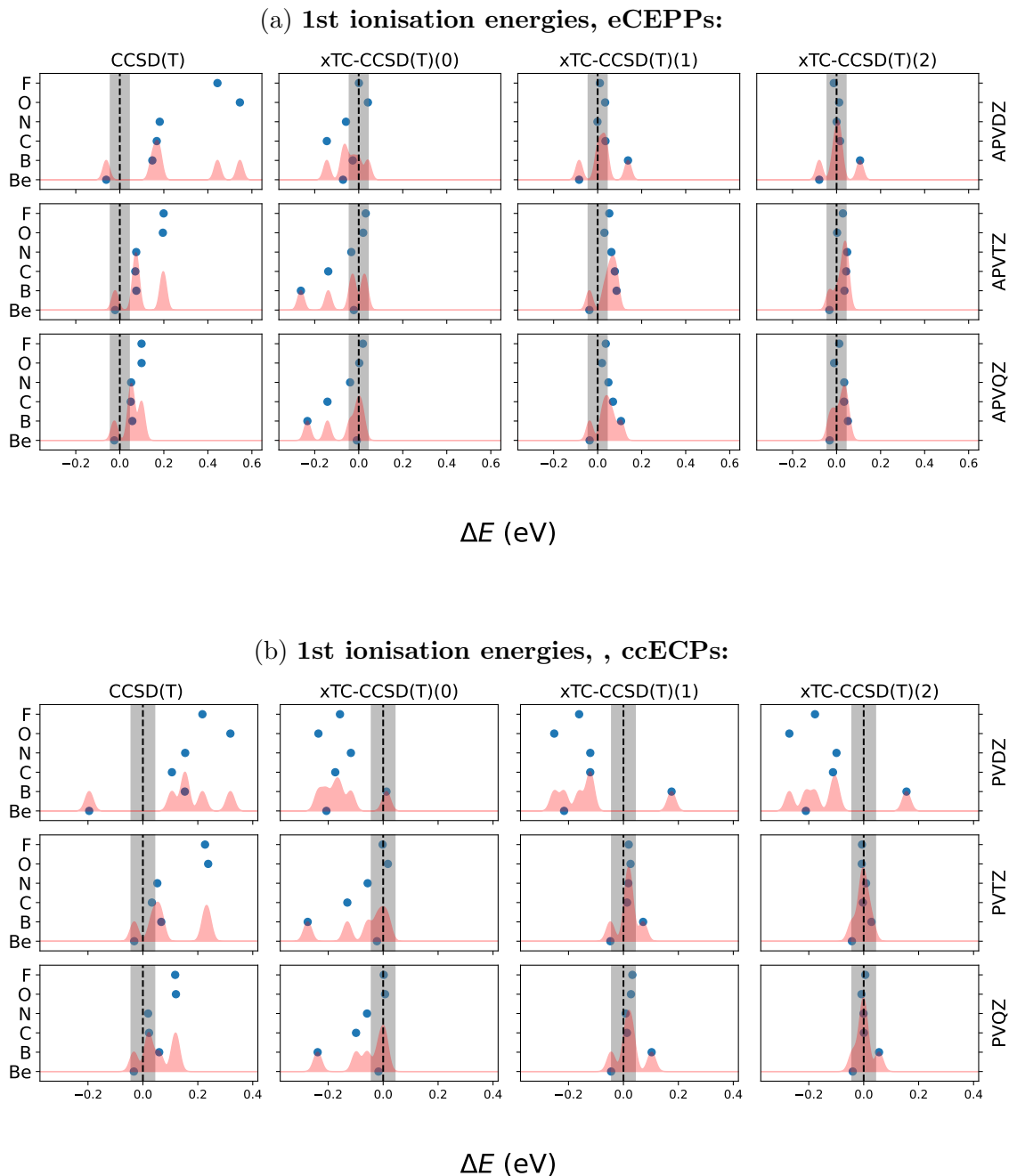


Figure 4: Ionisation energies (IPs)  $E_i = E_{\text{atom}} - E_{\text{ion}}$  for the first row elements, using (a) eCEPPs and (b) ccECPs. The energies are presented as the discrepancy with the experimental ionisation energies,<sup>39</sup> so that the presented energies are  $\Delta E = E_{\text{method}}^{\text{basis}} - E_{\text{exp}}$ . The X-axis shows the xTC-CCSD(T)(PP- $n$ ) ionisation energies with  $n = 0, 1, 2$  (in 2nd, 3rd, and 4th column, respectively). The 1st column shows CCSD(T) ionisation energies. The basis sets used are the AVXZ series for eCEPPs and the PVXZ series for ccECPs, where X is either D, T, or Q in the 1st, 2nd, and 3rd row, respectively. The grey shaded region denotes chemical accuracy. The red shading denotes a sum of gaussians, centered at each data point, with a width set such that equidistant gaussians in the presented scale would overlap at 95 % confidence.

It is interesting to note that xTC methods in double-zeta basis set are much better with eCEPPs than ccECPs, while the ccECPs are better with higher-order basis sets when  $n > 0$ . This phenomenon is not seen with standard CCSD(T), where the accuracy is similar with both PPs at the same basis set cardinal number. Another feature visible in this table is that the best results with xTC-CCSD(T) and ccECPs are obtained with the PVTZ basis set, and not with the PVQZ basis set, again when  $n > 0$ . This is not true with eCEPPs or with CCSD(T). With eCEPPs and xTC-CCSD(T)(PP-2) the results are converged in AVTZ basis.

When comparing the results with 2 and 3 commutators evaluated, the MAE and MSE are within 1 mHa. The 4th commutator produces practically identical results to the 3rd commutator.

Table 4: Mean absolute and root mean square errors (MAE and MSE) against the experimental ionisation energies of CCSD(T) and xTC-CCSD(T)(PP- $n$ ) methods with  $n = 0 - 4$ . Results are obtained with eCEPPs and ccECPs across different basis sets. The errors are in eV

# of comms.	Error	eCEPP (eV)			ccECP (eV)		
		AVDZ	AVTZ	AVQZ	PVDZ	PVTZ	PVQZ
CCSD(T)	MAE	0.2520	0.1001	0.0574	0.1846	0.1020	0.0560
	RMS	0.3047	0.1185	0.0624	0.1966	0.1330	0.0691
xTC-CCSD(T)(PP-0)	MAE	0.0630	0.0833	0.0737	0.1565	0.0899	0.0756
	RMS	0.0754	0.1234	0.1136	0.1724	0.1283	0.1099
xTC-CCSD(T)(PP-1)	MAE	0.0530	0.0520	0.0470	0.1803	0.0277	0.0338
	RMS	0.0694	0.0566	0.0568	0.1859	0.0371	0.0476
xTC-CCSD(T)(PP-2)	MAE	0.0435	0.0259	0.0266	0.1769	0.0191	0.0225
	RMS	0.0568	0.0303	0.0302	0.1858	0.0243	0.0296
xTC-CCSD(T)(PP-3)	MAE	0.0439	0.0267	0.0273	0.1772	0.0197	0.0231
	RMS	0.0574	0.0313	0.0314	0.1860	0.0251	0.0306
xTC-CCSD(T)(PP-4)	MAE	0.0439	0.0267	0.0272	0.1772	0.0197	0.0230
	RMS	0.0573	0.0312	0.0312	0.1860	0.0251	0.0306

To conclude this section, we have shown that it is necessary to include at least the second commutator, i.e. the PP-2 approximation, to achieve chemical accuracy in the ionisation

potentials of the first-row atoms with the xTC-CCSD(T)-PP- $n$  method. In other words, the first two non-zero commutators arising from the non-local pseudopotentials with the Jastrow factors are critically important to maintain reliability in the TC method with ECPs. Going to higher order commutators do not significantly change the results and hence can be disregarded. In further work we employ the PP-2 approximation.

# Molecules

## Total transcorrelated energies

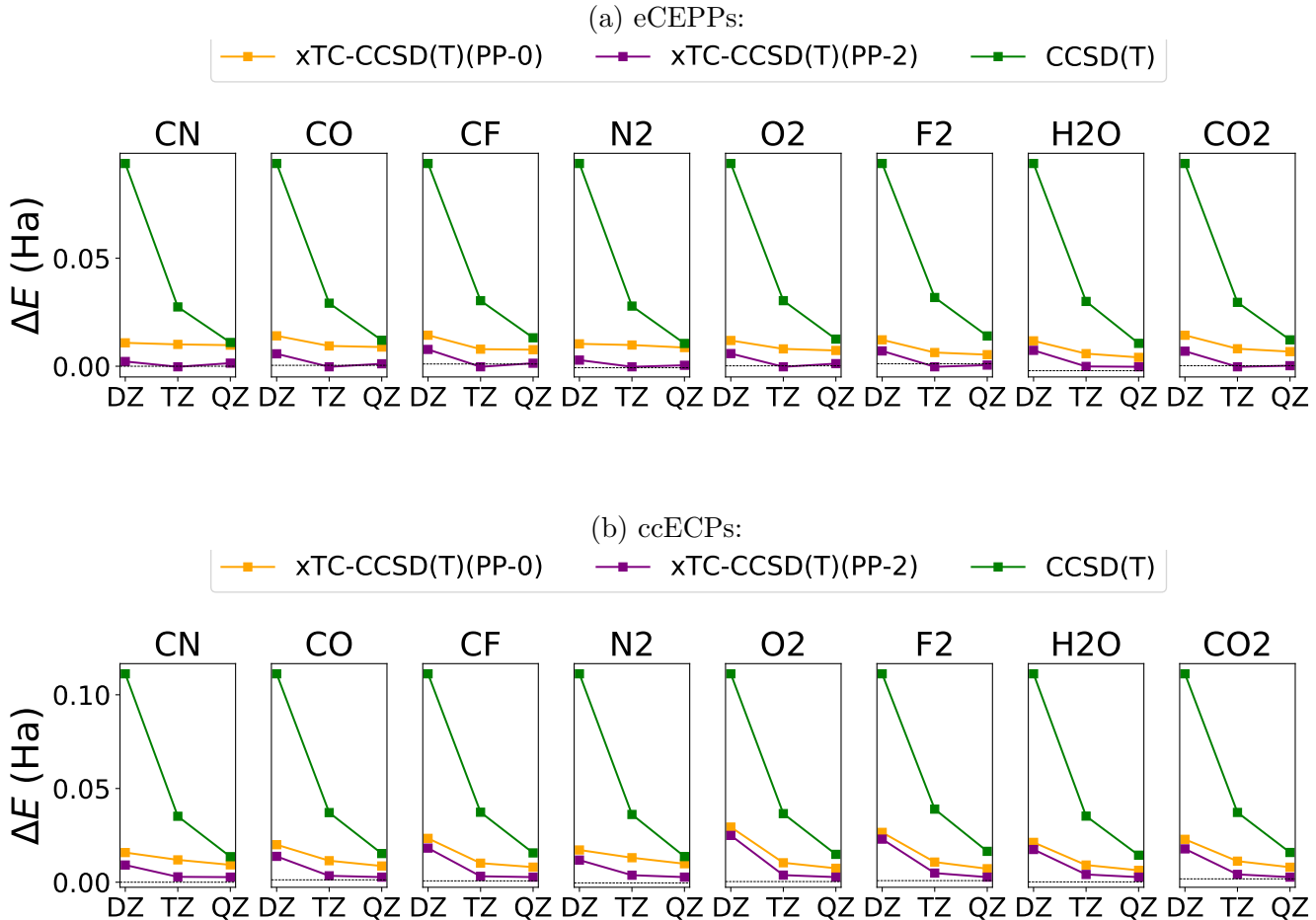


Figure 5: Energies of the molecules CN, CO, CF, N<sub>2</sub>, O<sub>2</sub>, F<sub>2</sub>, H<sub>2</sub>O, and CO<sub>2</sub> with eCEPPs (a) and ccECPs (b) as a function of the basis set. The energies are relative to CCSD(T) CBS energies as  $\Delta E = E - E_{\text{CBS}}^{\text{TZ-QZ}}(\text{CCSD(T)})$ , see Eq. (14). CCSD(T) (green), xTC-CCSD(T)(PP-0) (yellow), and xTC-CCSD(T)(PP-2) (violet) energies are shown.

Figure 5 shows the energies of the molecules CN, CO, CF, N<sub>2</sub>, O<sub>2</sub>, F<sub>2</sub>, H<sub>2</sub>O, and CO<sub>2</sub>, obtained with eCEPPs (a) and ccECPs (b) with CCSD(T) and xTC-CCSD(T)(PP-*n*) methods with *n* = 0 and *n* = 2. The energies are displayed relative to  $E_{\text{CBS}}^{\text{TZ-QZ}}(\text{CCSD(T)})$ . The results are shown as a function of the basis set.

The xTC energies are always below CCSD(T) energies at all basis sets. Evaluation of the PP commutators decreases the energies. Unlike with some atoms and ions, xTC-

CCSD(T)(PP-0) is still lower in energy than CCSD(T) for the molecules. The increase of the basis set size has a very small effect to the xTC-CCSD(T) energies compared to the basis-set dependence of CCSD(T) energies.

## F12 atomization energies

Figure 6 shows the atomization energies of the molecules CN, CO, CF, N<sub>2</sub>, O<sub>2</sub>, F<sub>2</sub>, H<sub>2</sub>O, and CO<sub>2</sub>, calculated with CCSD(T)-F12. The results are shown relative to the HEAT database.<sup>27</sup> The results are obtained with the AVXZ basis sets, with X=D,T,Q. The results are shown for all-electron, eCEPP, and ccECP calculations.

The all-electron CCSD(T)-F12 method shows excellent accuracy. With eCEPPs the accuracy is clearly worse, but then again with ccECPs all atoms are within chemical accuracy, except N<sub>2</sub>, which has a discrepancy of  $\sim 50$  meV.

Table 5 shows the MAE and RMS of the atomization energies of the molecules CN, CO, CF, N<sub>2</sub>, O<sub>2</sub>, F<sub>2</sub>, H<sub>2</sub>O, and CO<sub>2</sub>, obtained with CCSD(T)-F12 and MRCI-F12 methods. The errors are averaged over the molecules studied, and are shown separately for each basis set and core treatment. CCSD(T)-F12 is chemically accurate in AVTZ and AVQZ basis sets with all-electron calculations and with ccECPs both in terms of MAE and RMS.

The eCEPPs do not provide chemical accuracy. An interesting observation is that with eCEPPs the MAE and RMS decrease with increasing basis set accuracy, but that the best MAE and RMS with ECPs is obtained with the AVTZ basis set, and the AVQZ basis set is worse in MAE and almost equivalent in RMS. This decrease in accuracy with ccECPs when moving from triple to quadruple zeta basis was already seen with the ionisation energies of the first row elements and with the xTC-CCSD(T) method.



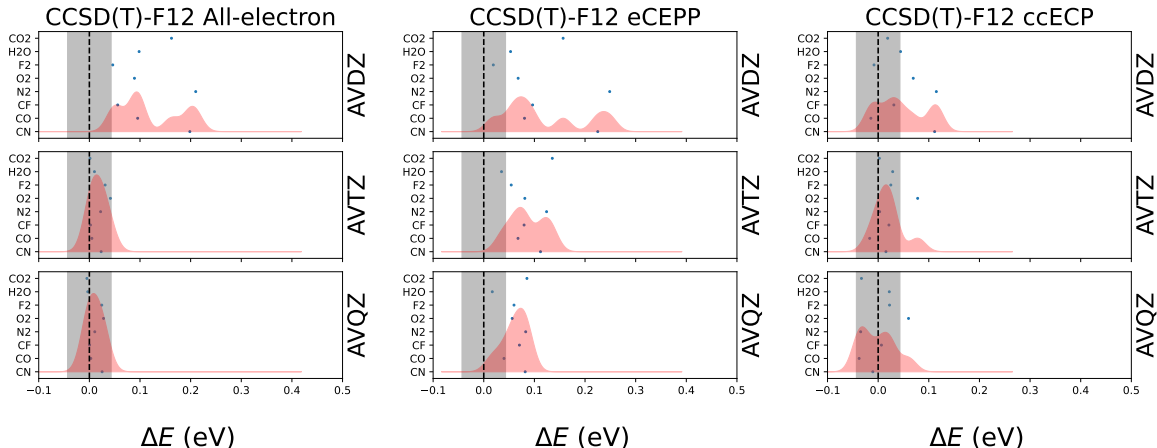


Figure 6: Atomization energies of the molecules CN, CO, CF, N<sub>2</sub>, O<sub>2</sub>, F<sub>2</sub>, H<sub>2</sub>O, and CO<sub>2</sub>, evaluated as  $E_{\text{at}} = \sum E_{\text{atom}} - E_{\text{mol}}$ , calculated with CCSD(T)-F12 method. The energies are presented relative to the results in the HEAT database, so that the presented energies are  $\Delta E = E_{\text{HEAT}} - E_{\text{at}}$ . Results are obtained using AVXZ basis sets, with X=D,T,Q (see labels on right). Results from all-electron (top), eCEPP (middle), and ccECP (bottom) calculations are shown. The grey shaded region denotes chemical accuracy. The red shading represents a sum of gaussians centered at the atomization energy discrepancies of each molecule, with sigmas set so that equidistantly placed gaussians over the interval between maximum and minimum of any calculation with a given core treatment (AE, eCEPP, ccECP) would have nearest-neighbour distance of 4 sigma.

Table 5: Mean average and root-mean square errors (MAE and RMS) of the CCSD(T)-F12 atomization energies of the molecules studied. The all-electron values, as well as ccECP and eCEPP pseudopotential results are shown.

Quantity	All-electron			eCEPP			ccECP		
	avdz	avtz	avqz	avdz	avtz	avqz	avdz	avtz	avqz
MAE	0.1133	0.0193	0.0135	0.1184	0.0861	0.0616	0.0515	0.0238	0.0283
RMS	0.1284	0.0235	0.0175	0.1417	0.0921	0.0656	0.0652	0.0326	0.0325

### Atomization energies with transcorrelation

We calculated the atomization energies of the molecules CN, CO, CF, N<sub>2</sub>, O<sub>2</sub>, F<sub>2</sub>, H<sub>2</sub>O, and CO<sub>2</sub>, using eCEPPs and ccECPs with AVXZ basis sets (Figures 7 and 8). The results are presented as discrepancies relative to the HEAT values,<sup>27</sup> employing CCSD(T) and CCSDT.<sup>30</sup> Both methods were applied in three variants: non-TC, xTC without PP

commutator evaluations, and xTC with two PP commutator evaluations.

### eCEPP Atomization energies with AVXZ

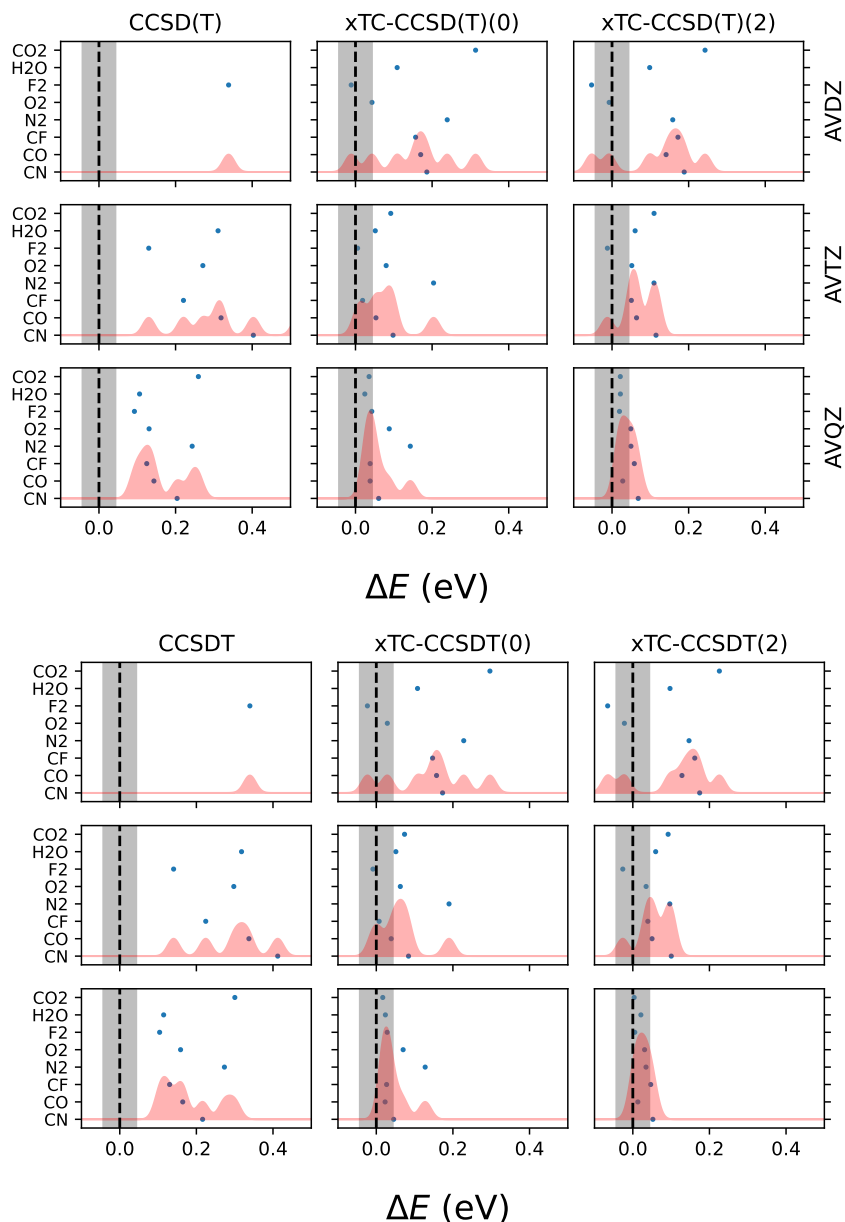


Figure 7: Atomization energies of a test set of molecules, evaluated with eCEPPs as  $E_{\text{at}} = \sum E_{\text{atom}} - E_{\text{mol}}$ . The energies are presented relative to the results in the HEAT database, so that the presented energies are  $\Delta E = E_{\text{HEAT}} - E_{\text{at}}$ . Calculations are shown without TC (left column), and with xTC both without and with 2 PP commutator evaluations ( $\{method\}(0)$  and  $\{method\}(2)$ ), respectively, method being either CCSD(T) or CCSDT). The grey shaded region denotes chemical accuracy. The red shading represents a sum of gaussians centered at the atomization energy discrepancies of each molecule, with sigmas set so that equidistantly placed gaussians over the interval between maximum and minimum of a given level of theory would have nearest-neighbour distance of 4 sigma. To improve presentation and to better compare with CCSD(T)-F12 results, we are only showing the region  $-0.1 < \Delta E < 0.5\text{eV}$ , which leaves some of the energies of non-transcorrelated methods outside of the range in AVDZ and AVTZ basis sets.

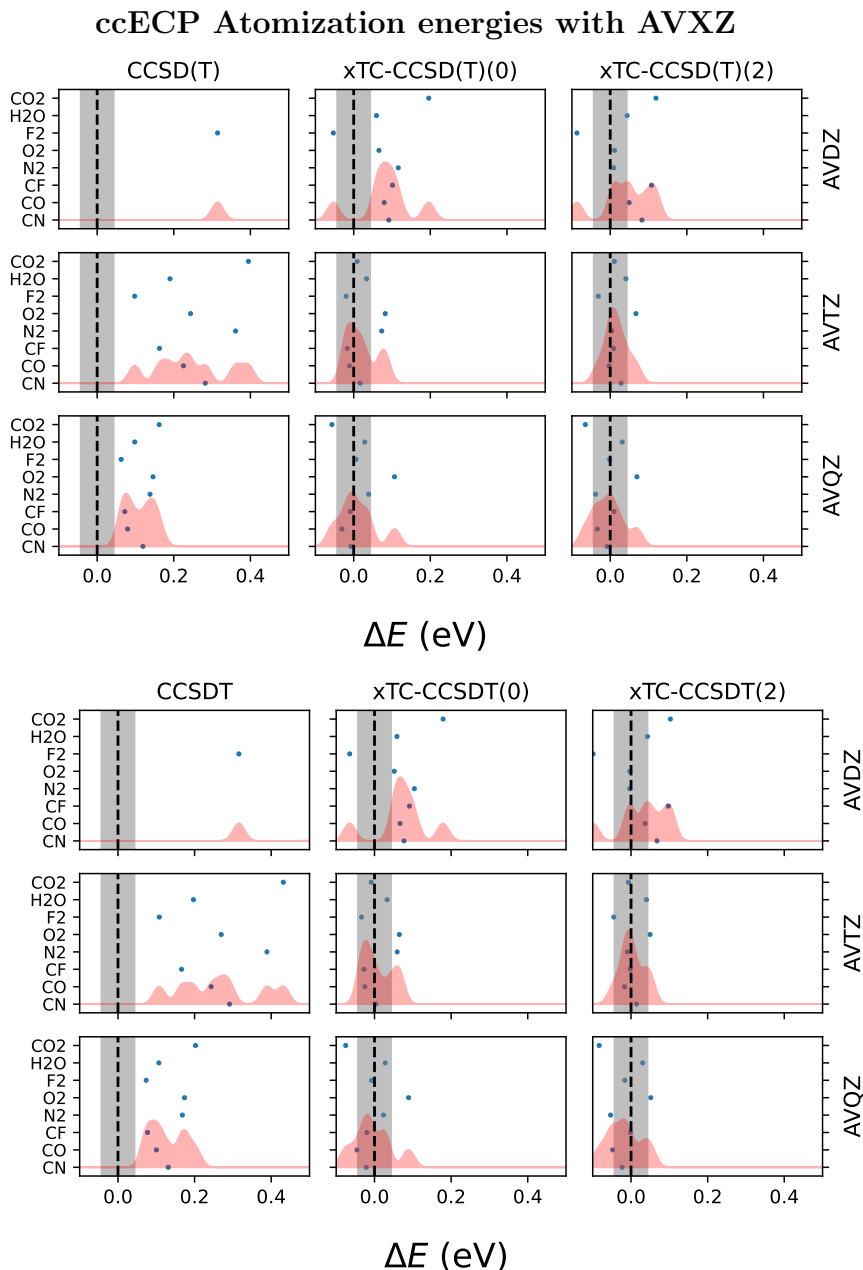


Figure 8: Results evaluated as in Fig. 7, but with ccECPs and AVXZ (X=D,T,Q) basis sets.

The eCEPP results (Figure 7) show consistent improvement in accuracy with basis set size. Both xTC variants outperform the non-TC calculations with both CCSD(T) and CCSDT, with PP commutator evaluations further enhancing accuracy. xTC-CCSDT(2) reaches chemical accuracy for all molecules studied. The results with ccECPs show best performance with xTC and ECP commutator evaluations in the AVTZ basis, where the

results are even more accurate than with eCEPPs in AVQZ basis. However, the ccECP results in AVQZ basis, despite being within chemical accuracy (with CO<sub>2</sub> slightly outside of the chemical accuracy regime), are slightly worsened from AVTZ results.

Table 6 summarizes the mean absolute errors (MAE) and root mean square errors (RMS) for all combinations of PP type, method, basis set, and theory. In terms of MAE and RMS, non-transcorrelated methods remain far from chemical accuracy even with the AVQZ basis set. In contrast, transcorrelated methods with eCEPPs, AVQZ basis sets, and two PP commutator evaluations achieve chemical accuracy across all studied methods. With ccECPs, xTC methods with two PP commutator evaluations are within or very close to chemical accuracy with AVQZ basis, and within chemical accuracy using the AVTZ basis set. The fact that we see best results with AVTZ basis, and not with AVQZ basis, when using ccECPs both with F12 and transcorrelated methods hints that the non-monotonic increase in accuracy with basis set resolution is a feature of the ccECPs.

## Dissociation energies

### N<sub>2</sub>

Figure 9 shows energy differences between experimental and theoretical evaluations of the N<sub>2</sub> dissociation curve. Energy differences are presented as a function of bond length. The experimental curve is taken from Ref.<sup>40</sup> The theoretical curves are evaluated with FCIQMC and MRCI methods. We used eCEPPs and did the calculations in AVDZ, AVTZ, and AVQZ basis sets using FCIQMC. We show results for FCIQMC and xTC-FCIQMC(PP-2). MRCI-F12 results are only evaluated in the AVQZ basis set. The theoretical results are shifted to overlap with experiment at  $r = 4.2 \text{ \AA}$ , a length which corresponds to the system of two isolated nitrogen atoms.

Table 6: Mean Absolute Errors (MAE) and Root Mean Square Errors (RMS) for Different Methods.

Method	MAE					
	eCEPP			ccECP		
	avdz	avtz	avqz	avdz	avtz	avqz
CCSD(T)	0.900	0.340	0.163	0.773	0.245	0.101
xTC-CCSD(T) (PP-0)	0.154	0.075	0.059	0.095	0.033	0.036
xTC-CCSD(T) (PP-2)	0.133	0.072	0.039	0.064	0.024	0.032
CCSDT	0.904	0.358	0.183	0.776	0.262	0.129
xTC-CCSDT (PP-0)	0.145	0.065	0.045	0.087	0.032	0.039
xTC-CCSDT (PP-2)	0.128	0.062	0.026	0.057	0.023	0.038

Method	RMS					
	eCEPP			ccECP		
	avdz	avtz	avqz	avdz	avtz	avqz
CCSD(T)	0.969	0.366	0.174	0.833	0.262	0.115
xTC-CCSD(T) (PP-0)	0.179	0.095	0.069	0.105	0.043	0.048
xTC-CCSD(T) (PP-2)	0.151	0.079	0.043	0.075	0.032	0.040
CCSDT	0.974	0.385	0.195	0.837	0.281	0.137
xTC-CCSDT (PP-0)	0.169	0.084	0.057	0.095	0.038	0.047
xTC-CCSDT (PP-2)	0.141	0.068	0.031	0.069	0.030	0.045

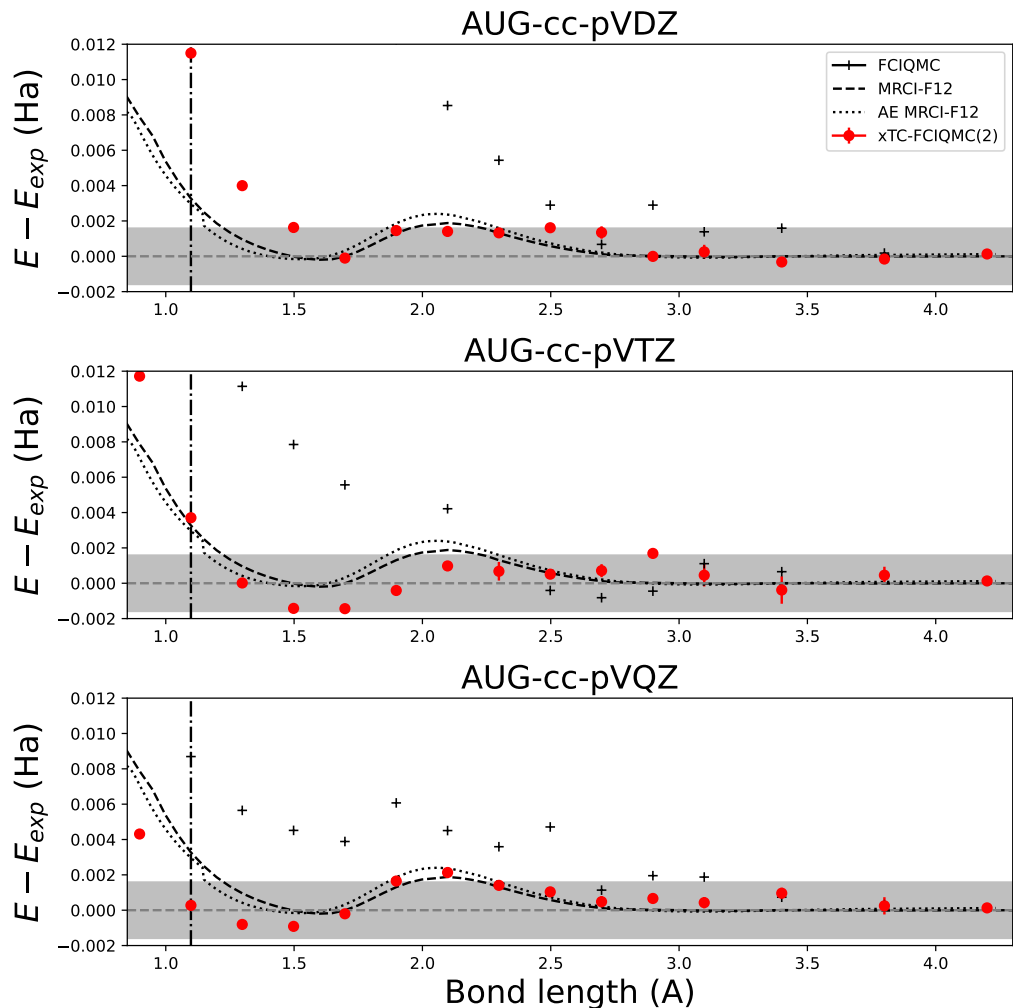


Figure 9:  $N_2$  FCIQMC (black crosses) and xTC-FCIQMC(PP-2) (red circles) dissociation curves as a function of bond length with eCEPPS, computed in AVDZ (top row), AVTZ (middle row) and AVQZ (bottom row) basis sets. MRCI-F12 energies are evaluated in AVQZ basis set in all of the images, and both eCEPP (dashed black) and all-electron MRCI-F12 (dotted black) curves are shown. MRCI-F12 results are evaluated in the AVQZ basis set in all of the images. Results are presented as differences to experimental dissociation curve from Ref.<sup>40</sup> taking the overlap between theory and experiment to be at  $r = 4.2$  Å. The grey shaded region denotes chemical accuracy with respect to experiment. The dash-dotted vertical line points to the equilibrium bond length of  $N_2$  of  $r = 1.098$  Å.

Because of the strong correlations and change of spin state involved in dissociation of the  $N_2$ , the Hartree-Fock wave function is a poor reference for the Jastrow factor optimization. Hence we used a method developed recently to tackle this problem.<sup>41</sup> First, we took the 100 most populated determinants from a non-transcorrelated FCIQMC calculation, and used

them for constructing a trial wave function for VMC, and optimized the Jastrow factor with the VMC method before using it for preparing the transcorrelated Hamiltonian. In the subsequent xTC phase we used the reduced density matrix of the multideterminant wave function used in the optimisation.

Figure 9 shows that the regular (non-transcorrelated) FCIQMC does not achieve chemical accuracy with respect to basis-set-error at near-equilibrium bond lengths. xTC-FCIQMC(PP-2) underestimates the equilibrium energy at triple-zeta basis by about 4mH, but has an excellent match in quadruple zeta-basis, a feature already seen with xTC coupled cluster methods and eCEPPs in Fig. 7. The xTC-FCIQMC(PP-2) method in quadruple zeta-basis obtains chemical accuracy everywhere except at the most compressed bond length (below 1Å), and at  $r = 2.098 \text{ Å}$ , where, however, the stochastic error of the result overlaps with chemical accuracy regime.

We tested the size-consistency by calculating the difference between the FCIQMC energies of two isolated nitrogen atoms and the energy of the  $\text{N}_2$  molecule at the longest bond distance studied,  $\Delta E = 2E_{\text{N}} - E_{\text{N}_2}(r = 4.2\text{Å})$ . This test was done in AVDZ basis, and resulted in  $\Delta E = -1.5(2)\text{mHa}$ . This small size-inconsistency can be traced to the use of the combined Jastrow treatment (see discussion after Eq. (6)) together with the xTC approximation, since the latter approximates the effect of the three-body interactions introduced by the commutators of the kinetic energy operator and the Jastrow factor. In the combined Jastrow approach the one-body terms are folded into 2-body Jastrow terms, which in turn leads to additional 3-body interactions (approximated in the xTC treatment). This combination leads to size-inconsistency. This size-consistency error can be entirely eliminated by using the separated Jastrow treatment (See Supplementary material for the separate treatment of PP commutators). We verified explicitly with further calculations that the xTC approximation, in the separate Jastrow treatment, does not incur a size-consistency error. Because we checked that in equilibrium geometries the separate and combined treatments yielded the same results, the overall error in this study due to the aforementioned size-inconsistency is on



the order of 1-2mHa. The best workflow for future studies will require further investigation of Jastrow cutoffs and the use of the separate Jastrow treatment.

The MRCI-F12 results are in good agreement with the experimental curve at longer distances, but overestimate the energy at equilibrium distance. The correspondence between the eCEPP and all-electron curves indicate that the eCEPPs introduce almost no error into the simulation.

## **F<sub>2</sub>**

Figure 10 shows the dissociation error curve of F<sub>2</sub>, showing the difference between MRCI-F12 and xTC-FCIQMC(PP-2) theoretical methods and experiment. xTC-FCIQMC(PP-2) results are evaluated with eCEPPS and computed in AVDZ, AVTZ, and AVQZ basis sets. The MRCI-F12 results are evaluated in the AVQZ basis set. The experimental curve is taken from Ref.<sup>42</sup> Because the experimental data extends only to  $r \sim 2.8$  Å, the theoretical results are shifted to overlap with experiment at the equilibrium bond length of  $r = 1.4118$  Å.

The Jastrow factors for F<sub>2</sub> are optimized with only the RHF determinant in the VMC method. This proves to be already highly accurate, as for F<sub>2</sub> only a single bond is broken and less correlation is involved in the dissociation.

The xTC-FCIQMC(PP-2) results at triple zeta and higher basis sets are very accurate, with a sub-mHa error along the whole range of the plot with AVQZ basis set. MRCI-F12 are also chemically accurate with the AVQZ basis set, but the error is larger.

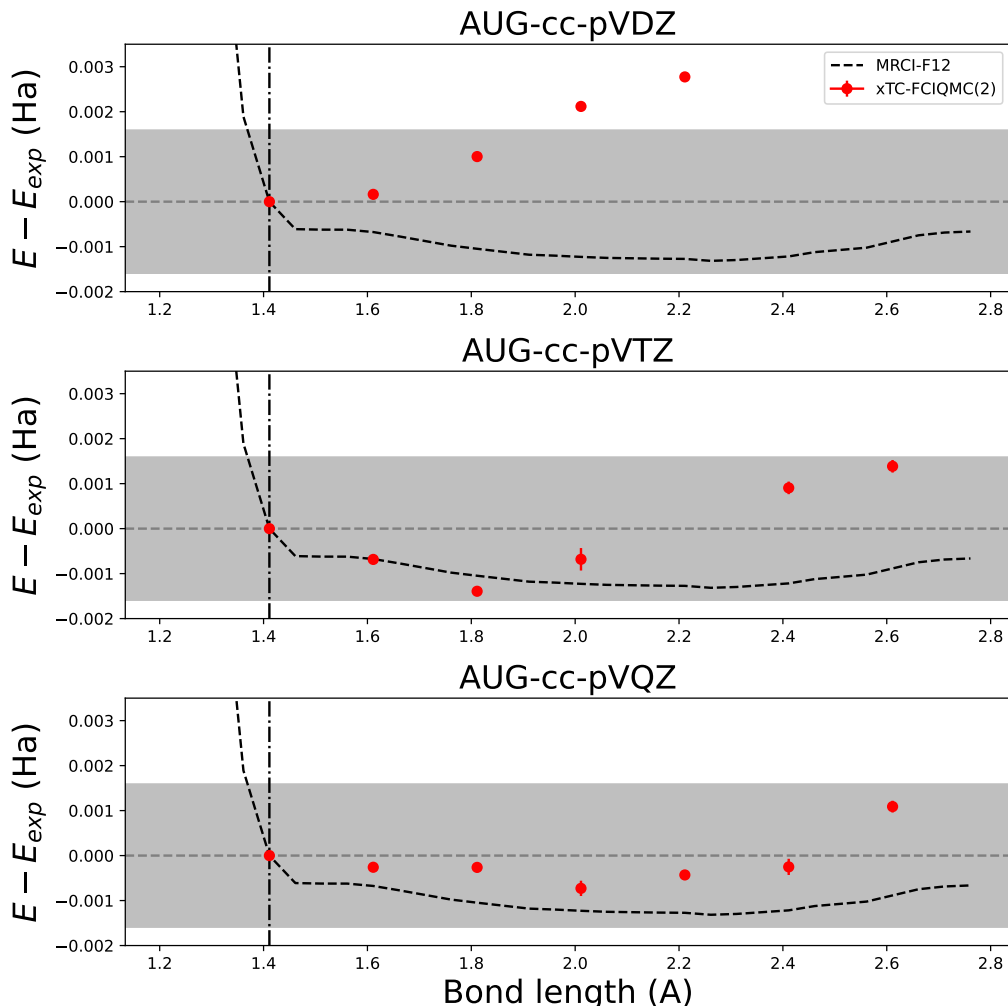


Figure 10:  $\text{F}_2$  xTC-FCIQMC(PP-2) and MRCI-F12 energies as a function of bond length with eCEPPS, computed in AVDZ (top row), AVTZ (middle row) and AVQZ (bottom row) basis sets. MRCI-F12 energies are the same in all plots, and are evaluated in AVQZ basis set. Results are presented as differences to experimental dissociation curve from Ref.<sup>42</sup> The grey shaded region denotes the chemical accuracy with respect to experiment. The dotted vertical line points to the equilibrium bond length of  $\text{F}_2$  of 1.4112 Å.

## Conclusions

We have presented a study of transcorrelated theory under PP approximations. The study included the derivation of the PP commutators needed for evaluating the transcorrelated Hamiltonian. The algorithms were implemented using an in-house code TCHINT, that was subsequently used to evaluate the accuracy of the transcorrelated methods with PPs.

The accuracy of the method was evaluated by estimating the ionisation potentials of atoms in the first row, the atomization energies of a test set of molecules, and the dissociation curves of  $\text{N}_2$  and  $\text{F}_2$ . The results were compared to the HEAT database, experimental data, and MRCI-F12 results.

xTC-CCSD(T)(PP-2) provided chemical accuracy for the ionisation energies of the first row atoms with both eCEPPs and ccECPs. For the atomization energies, all of the coupled cluster levels of theory with 2 PP commutator evaluations reached chemical accuracy with eCEPPs and AVQZ basis set. With ccECPs, chemical accuracy was reached with AVTZ basis set, while with AVQZ basis the RMS of the methods was slightly outside the chemical accuracy regime.

Atomization energy calculations with CCSD(T)-F12 showed the same trend of reduced accuracy when moving from AVTZ to AVQZ basis. This leads to the conclusion that with explicitly correlated methods, the ccECPs have some problems with augmented basis set convergence, but that the results are very accurate already at triple-zeta level. The F12 methods were found to work better with ccECPs than eCEPPs.

Finally, the dissociation curves of  $\text{N}_2$  and  $\text{F}_2$  were evaluated with xTC-FCIQMC and MRCI-F12 methods. The xTC-FCIQMC results were very accurate with the AVQZ basis set, and apart from the compressed distance region of  $\text{N}_2$ , chemical accuracy was reached.

The results of this study show that the transcorrelated methods are very accurate with PPs, and that the accuracy is comparable to the all-electron results. The evaluation of the PP commutators is essential for the accuracy of the method. It is possible that optimisation of the Jastrow factor without the presence of the core electrons allows a more targeted TC simulation, focusing on the valence electrons, a feature that can provide useful in the future development of the method.

The theory of transcorrelation with PPs can help bringing the applicability of the TC method to a wider range of systems. Calculations with larger system sizes can benefit from the reduced variance, making the Jastrow optimizations more feasible. Applications with

heavier atoms, such as transition metals, would be an interesting future direction. Crucially, the methods presented in this work can help in the development of TC theory towards periodic solid-state systems, possibly even in the plane-wave basis. Directions towards application of TC theory with PPs in embedding models for systems such as solid-state defects are also currently under investigation.

## Supporting Information

Supporting Information. • Optimized Jastrow factor parameters for atoms and molecules studied in this work. • Derivations of pseudopotential commutator formulas (separate Jastrow treatment). • FCIDUMP files containing transcorrelated second-quantized Hamiltonians for Be in AVDZ basis set, with and without the PP commutator evaluations.

## References

- (1) Kato, T. On the eigenfunctions of many-particle systems in quantum mechanics. *Communications on Pure and Applied Mathematics* **1957**, *10*, 151–177.
- (2) Kutzelnigg, W. r 12-Dependent terms in the wave function as closed sums of partial wave amplitudes for large l. *Theoretica chimica acta* **1985**, *68*, 445–469.
- (3) Ten-no, S. Initiation of explicitly correlated Slater-type geminal theory. *Chemical Physics Letters* **2004**, *398*, 56–61.
- (4) Kutzelnigg, W.; Klopper, W. Wave functions with terms linear in the interelectronic coordinates to take care of the correlation cusp. I. General theory. *The Journal of Chemical Physics* **1991**, *94*, 1985–2001.
- (5) Noga, J.; Kutzelnigg, W. Coupled cluster theory that takes care of the correlation cusp by inclusion of linear terms in the interelectronic coordinates. *The Journal of Chemical Physics* **1994**, *101*, 7738–7762.
- (6) Kong, L.; Bischoff, F. A.; Valeev, E. F. Explicitly Correlated R12/F12 Methods for Electronic Structure. *Chemical Reviews* **2012**, *112*, 75–107.
- (7) Cohen, A. J.; Luo, H.; Guthrie, K.; Dobrautz, W.; Tew, D. P.; Alavi, A. Similarity transformation of the electronic Schrödinger equation via Jastrow factorization. *The Journal of Chemical Physics* **2019**, *151*, 061101.
- (8) Ammar, A.; Scemama, A.; Giner, E. Transcorrelated selected configuration interaction in a bi-orthonormal basis and with a cheap three-body correlation factor. *The Journal of Chemical Physics* **2023**, *159*, 114121.
- (9) Ammar, A.; Scemama, A.; Giner, E. Biorthonormal Orbital Optimization with a Cheap Core-Electron-Free Three-Body Correlation Factor for Quantum Monte Carlo and

- Transcorrelation. *Journal of Chemical Theory and Computation* **2023**, *19*, 4883–4896, PMID: 37390472.
- (10) Lee, N.; Thom, A. J. W. Studies on the Transcorrelated Method. *Journal of Chemical Theory and Computation* **2023**, *19*, 5743–5759, PMID: 37640393.
  - (11) Ten-no, S. L. Nonunitary projective transcorrelation theory inspired by the F12 ansatz. *The Journal of Chemical Physics* **2023**, *159*, 171103.
  - (12) Ammar, A.; Scemama, A.; Loos, P.-F.; Giner, E. Compactification of determinant expansions via transcorrelation. *The Journal of Chemical Physics* **2024**, *161*, 084104.
  - (13) Haupt, J. P.; Hosseini, S. M.; López Ríos, P.; Dobrautz, W.; Cohen, A.; Alavi, A. Optimizing Jastrow factors for the transcorrelated method. *The Journal of Chemical Physics* **2023**, *158*, 224105.
  - (14) Dobrautz, W.; Luo, H.; Alavi, A. Compact numerical solutions to the two-dimensional repulsive Hubbard model obtained via nonunitary similarity transformations. *Phys. Rev. B* **2019**, *99*, 075119.
  - (15) Christlmaier, E. M. C.; Schraivogel, T.; López Ríos, P.; Alavi, A.; Kats, D. xTC: An efficient treatment of three-body interactions in transcorrelated methods. *The Journal of Chemical Physics* **2023**, *159*, 014113.
  - (16) Luo, H.; Alavi, A. Combining the Transcorrelated Method with Full Configuration Interaction Quantum Monte Carlo: Application to the Homogeneous Electron Gas. *Journal of Chemical Theory and Computation* **2018**, *14*, 1403–1411, PMID: 29431996.
  - (17) Liao, K.; Schraivogel, T.; Luo, H.; Kats, D.; Alavi, A. Towards efficient and accurate ab initio solutions to periodic systems via transcorrelation and coupled cluster theory. *Phys. Rev. Res.* **2021**, *3*, 033072.

- (18) Guthrie, K.; Cohen, A. J.; Luo, H.; Alavi, A. Binding curve of the beryllium dimer using similarity-transformed FCIQMC: Spectroscopic accuracy with triple-zeta basis sets. *The Journal of Chemical Physics* **2021**, *155*, 011102.
- (19) Schraivogel, T.; Cohen, A. J.; Alavi, A.; Kats, D. Transcorrelated coupled cluster methods. *The Journal of Chemical Physics* **2021**, *155*, 191101.
- (20) Schraivogel, T.; Christlmaier, E. M. C.; López Ríos, P.; Alavi, A.; Kats, D. Transcorrelated coupled cluster methods. II. Molecular systems. *The Journal of Chemical Physics* **2023**, *158*, 214106.
- (21) Sokolov, I. O.; Dobrutz, W.; Luo, H.; Alavi, A.; Tavernelli, I. Orders of magnitude increased accuracy for quantum many-body problems on quantum computers via an exact transcorrelated method. *Phys. Rev. Res.* **2023**, *5*, 023174.
- (22) Trail, J. R.; Needs, R. J. Shape and energy consistent pseudopotentials for correlated electron systems. *The Journal of Chemical Physics* **2017**, *146*, 204107.
- (23) Bennett, M. C.; Melton, C. A.; Annaberdiyev, A.; Wang, G.; Shulenburger, L.; Mitas, L. A new generation of effective core potentials for correlated calculations. *The Journal of Chemical Physics* **2017**, *147*, 224106.
- (24) Fahy, S.; Wang, X. W.; Louie, S. G. Variational quantum Monte Carlo nonlocal pseudopotential approach to solids: Formulation and application to diamond, graphite, and silicon. *Phys. Rev. B* **1990**, *42*, 3503–3522.
- (25) Drummond, N. D.; Towler, M. D.; Needs, R. J. Jastrow correlation factor for atoms, molecules, and solids. *Phys. Rev. B* **2004**, *70*, 235119.
- (26) TCHINT, To be published.

- (27) Tajti, A.; Szalay, P. G.; Császár, A. G.; Kállay, M.; Gauss, J.; Valeev, E. F.; Flowers, B. A.; Vázquez, J.; Stanton, J. F. HEAT: High accuracy extrapolated ab initio thermochemistry. *The Journal of Chemical Physics* **2004**, *121*, 11599–11613.
- (28) Sun, Q. et al. Recent developments in the PySCF program package. *The Journal of Chemical Physics* **2020**, *153*, 024109.
- (29) Needs, R. J.; Towler, M. D.; Drummond, N. D.; López Ríos, P.; Trail, J. R. Variational and diffusion quantum Monte Carlo calculations with the CASINO code. *The Journal of Chemical Physics* **2020**, *152*, 154106.
- (30) Kats, D.; Schraivogel, T.; Hauskrecht, J.; Rickert, C.; Wu, F., et al. ElemCo.jl: Julia program package for electron correlation methods. **2024**,
- (31) Kats, D.; Christlmaier, E. M.; Schraivogel, T.; Alavi, A. Orbital optimisation in xTC transcorrelated methods. *Faraday Discussions* **2024**, *254*, 382–401.
- (32) Werner, H.-J.; Knowles, P. J.; Knizia, G.; Manby, F. R.; ; Schütz, M. Molpro: a general-purpose quantum chemistry program package. *Wiley Interdisciplinary Reviews: Computational Molecular Science*
- (33) Werner, H.-J.; Knowles, P. J.; Manby, F. R.; Black, J. A.; Doll, K.; Heß, A., elmann; Kats, D.; Kö, A., hn; Korona, T.; Kreplin, D. A., et al. The Molpro quantum chemistry package. *The Journal of chemical physics* **2020**, *152*.
- (34) Werner, H.-J.; Knowles, P. J., et al. MOLPRO, a package of ab initio programs. *For more information, see <https://www.molpro.net/>,.*
- (35) Peterson, K. A.; Adler, T. B.; Werner, H.-J. Systematically convergent basis sets for explicitly correlated wavefunctions: The atoms H, He, B–Ne, and Al–Ar. *The Journal of Chemical Physics* **2008**, *128*, 084102.



- (36) Cleland, D.; Booth, G. H.; Alavi, A. Communications: Survival of the fittest: Accelerating convergence in full configuration-interaction quantum Monte Carlo. *The Journal of Chemical Physics* **2010**, *132*, 041103.
- (37) Guthrie, K. et al. NECI: N-Electron Configuration Interaction with an emphasis on state-of-the-art stochastic methods. *The Journal of Chemical Physics* **2020**, *153*, 034107.
- (38) Davidson, E. R.; Silver, D. W. Size consistency in the dilute helium gas electronic structure. *Chemical Physics Letters* **1977**, *52*, 403–406.
- (39) Chakravorty, S. J.; Gwaltney, S. R.; Davidson, E. R.; Parpia, F. A.; p Fischer, C. F. Ground-state correlation energies for atomic ions with 3 to 18 electrons. *Phys. Rev. A* **1993**, *47*, 3649–3670.
- (40) Le Roy, R. J.; Huang, Y.; Jary, C. An accurate analytic potential function for ground-state N<sub>2</sub>, from a direct-potential-fit analysis of spectroscopic data. *The Journal of Chemical Physics* **2006**, *125*, 164310.
- (41) Haupt, J. P.; *et al.*, To be published.
- (42) Colbourn, E. A.; Dagenais, M.; Douglas, A. E.; Raymond, J. W. The electronic spectrum of F<sub>2</sub>. *Canadian Journal of Physics* **1976**, *54*, 1343–1359.

# TOC Graphic

